

Investigation of the loads and the rise of tensile forces in sideflexing sliderail chains

DR.-ING. P. AUERBACH

PROF. DR.-ING. K. NENDEL

TU CHEMNITZ, PROFESSORSHIP OF CONVEYING ENGINEERING

Depiction of an analysis of the loads and stress distribution in sideflexing chains revolving in 3D-conveyor systems. The article describes the results of measurements of chain tensile forces under different loads and in different conveyor sections. Consecutively new equations for the tension rise in sliding curves are developed and compared to the measurements.

1 Introduction

Conveyor systems using sideflexing sliderail chains made of polymers are used in many branches for transporting light piece goods (< 20 kg). Their advantages include the form-locking, slippage free drive, the possibility for clean, lubrication-free operation and the sideflexing as well as rebending degrees of freedom allowing for horizontal and vertical curves. Conveyor systems for these chains are built up from a number of modules, that can be combined freely to form a multitude of possible, spatial conveyor layouts for nearly any kind of transportation task (Figure 1).

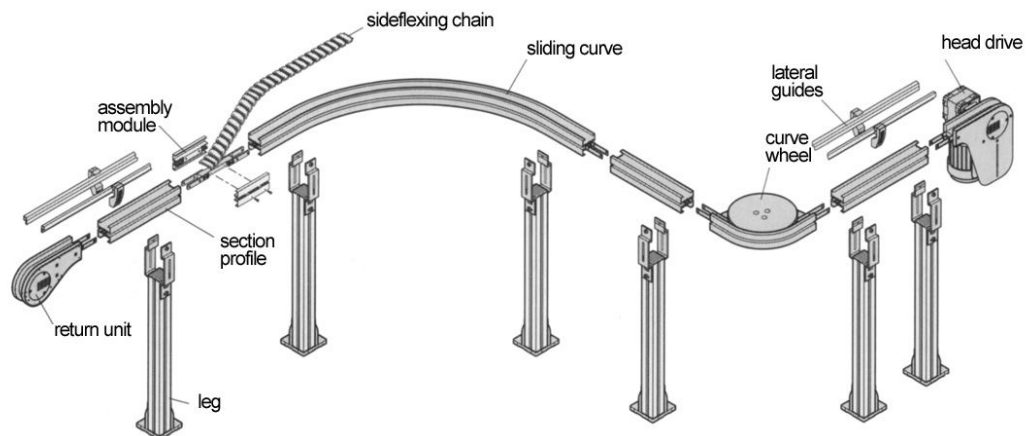


Fig. 1: Components of a chain conveyor system [Bosch04]

Despite the widespread use of these conveyor systems, the knowledge about the mechanical loads, their durability and dimensioning is still rather incomplete. The relevant literature contains virtually no information referring to these problems. The simplified equations, given in the engineering manuals of the manufacturers of these systems, allow only for a roughly estimated dimensioning of the chains but give no clue about their durability. For a parameter, which is describing the stability, solely the static breaking load of a chain will be consulted and afterwards it will be divided through a safety factor between three and four. Long-term tests showed, that the slide chains, depending on the conveyor layout, only achieve a very small durability (e.g. below 500 h), if the traction force comes close to the allowable traction, that has been calculated in this manner. Furthermore, the reached durability is strongly depending on how many curves the conveyor includes.

To achieve a better understanding about the strain and the character of fatigue-life of plastic slide chains, different examinations (in both areas) have been accomplished at the Professorship of Conveying Engineering at the Chemnitz University of Technology. The results will be published in two consecutive articles. The present article illustrates the results, which have been achieved while analysing the strains and the measurement as well as the exact mathematical description of chain traction. The second publication is concerned with the evaluation of fatigue strength data of plastic slide chains and proposes an approach, which allows an estimation of their durability. Furthermore, a calculation program, based on the gained data and equation, will be introduced, which permits a faster and more reliable design of slide chain conveyor systems.

2 Stress model

Unlike other kinds of chains respectively belts, side-flexing slide chains cannot only be turned around vertically but also horizontally. Different elements of the conveying system (straight line, drive, horizontal and vertical curves, etc.) create different kinds of stress onto the chain links. For a better understanding a stress model has been established for each element. All forces which affect a chain link have been applied in the following 3D-model. Considering as example for straight sections and horizontal curves, this is shown in figures two and three.

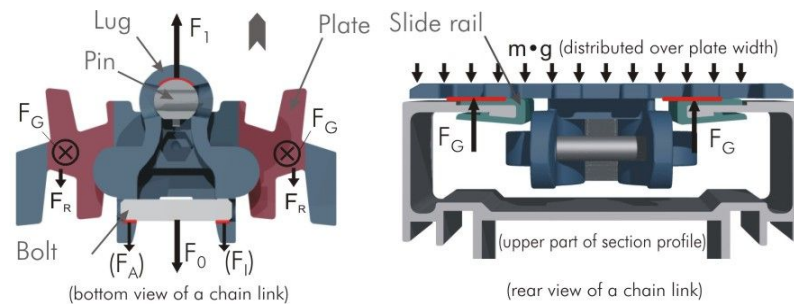


Fig. 2: Stress model for a straight track section

The figure shows, that a multitude of three-dimensional distributed forces acts on the chain links, but they clearly distinguish in absolute value. With the help of exemplary calculations with typical parameters for coefficient of friction, dimensions and weight of products as well as the weight of the chain, could be shown, that the chain traction force (F_I) is by far the largest force. Other forces, which are mainly evoked through the weight of the transported material and the chain as well as the friction on different contact points to the conduction system, are negligible smaller compared to the chain traction force. This can also be justified in the way that the maximum chain force is the total of many comparatively small friction forces on all chain links of the conduction system. Therefore, one can assume that a chain link in straight sections is subordinate to an uni-axial stress condition.

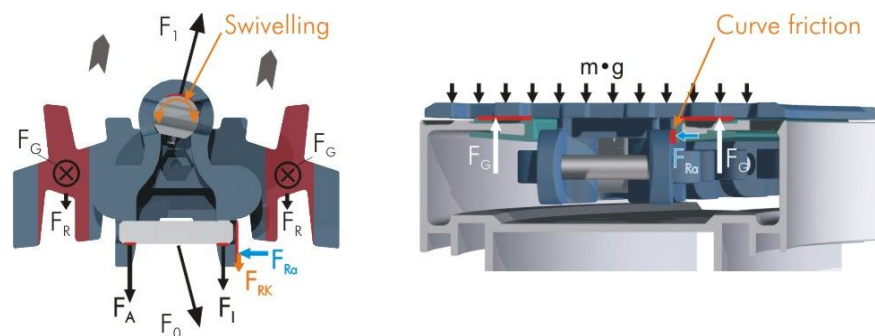


Fig. 3: Stress model horizontal curve

The force model of horizontal curves shows a major difference to the model of straight sections: the tractions on both sides of a chain link F_I and F_0 are not on the same line of action, but are rather pitched in a certain angle to each other. To pass through the curve, the chain links need to contort sidewise around that angle. The resulting radial force component F_{Ra} causes an additional friction force in the curve F_{RK} at the contact point to the ligament of the slide rail. Thereby the chain link will be loaded asymmetrically.

An even more intensive asymmetric stress develops at the interface between straight line and curve. At the side-flexing pivoting of the preceding chain link into the curve and back out again, the pin, which is sliding mounted in the leading part of the chain link (lug), will be contorted with full stress through the chain traction force. Thereby, a friction torque respectively a friction force emerges at the lug of the chain, temporarily. Thus, a friction torque respectively a friction force derives directly, in combination with the coefficient of friction between pin and chain, from the chain traction force and therefore reaches a significant value. That means, regarding the condition of stress, that a chain link is succumbed by a multiaxial stress during the passing through of curve sections, but especially at the transition between straight line and curve.

3 FEM-Analysis of the stresses

For the determination of the distribution and the maximum of the caused tensions in the chain link, FEM-simulations have been accomplished for the mentioned stress models. Contact-conditions between pin, bolt and slide bar have been included in the calculation, for the reason of a more detailed modelling of the power transmission onto the chain link. The load has been applied in defining the bolt as fixed element and in applying traction of 1.200 N at the pin. The relatively small friction force has been neglected in the simulation.

As one can recognize in Figure 4, clear differences are becoming apparent when comparing the calculated tension distribution for straight sections and curves as well as the transition between straight lines and curves. In case of an uniaxial stress, which is representing the stress in straight sections, a symmetric deformation and friction force is positioning itself, expectedly. The front part of the chain link starts deforming as soon as it enters the curve towards the centre of the chain link due to the radial element of the lean traction at the pin. The plate, which turns away from the curve, will be stressed even more.

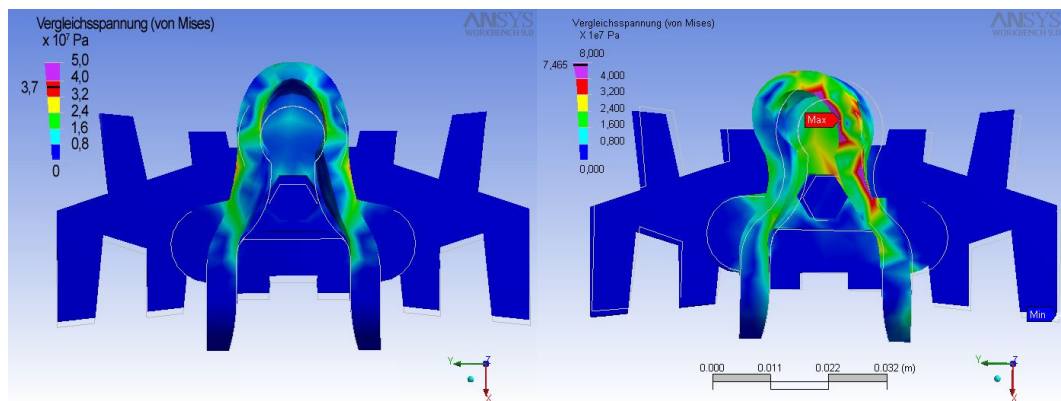


Fig. 4: Van-Mises-equivalent stress (LTR: straight, curve, transition)

As soon as the pin swivels in, which has been modelled as an additional force towards the curve center at the lug of the chain, the outer part of the link will be stressed even more. Not only appear higher maximum values of the equivalent stress, but also the size of highly stressed areas around the recess for the bolt in front of the link is increasing.

The results of the simulation emphasise, that a chain link in curves, especially in the transition from curve into straight section, is considerably more stressed than in straight sections only. Unlike the simulation, the stress of the chain during the passing through of a conveyor is not static, but time-variant. In doing so, every circulation means a tumescent change of load which damages the chain. If the conveyor includes curves, the chain will be damaged more than in exclusively straight sections. This has just been demonstrated through the increased stress in curve sections. The stability resources of the chain will be exhausted quicker, so that the durability, meaning the number of circulation until the fracture, will be considerably reduced because of curves. This conclusion will be certified in [Auerbach06], which describes the results of fatigue strength researches on plastic-slide chains in test-conveying systems.

4 Examination of chain traction force

To examine the mentioned, time-variant progression of the chain traction force, an appropriate system for the measurement and transmission of the force during the rotation of the chain had to be developed. The most important component of the same is the measuring chain link, which has been produced by modifying a standard chain link. For that purpose, the steel bolt has been drilled out, grinded on two opposite sides and provided with strain gauge. The standard pin was replaced by a modified equivalent with a hole and the chain plate was drilled as well to make room for the wiring. Subsequent, the electronics for the supply of the bridge driving voltage as well as the digitalisation and wireless transmission of the measured values to a computer had to be developed. This could be integrated in a very compact body, which was installed onto the chain and could circulate with it through the conveyor. With this measuring system (Figure 5) conveying systems could be analysed, which covered changing combination of all known components of routing (straight line, degree of arc, horizontal and vertical sliding roadway arch, drive and deflection), at different conveying speed and strain by material being conveyed.

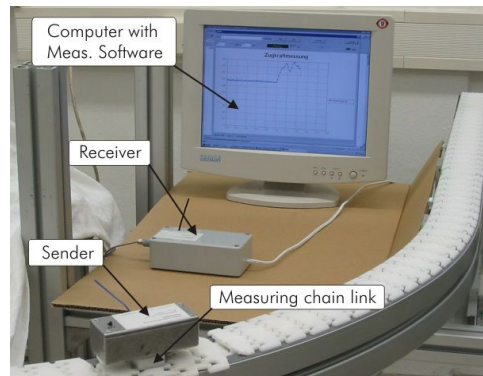


Fig. 5: Tension force measurement system

There it became clear, that the chain traction force shows following categorical characteristics when passing through a complete circulation of the conveyor: it is increasing continuously from the sapless condition in the chain-bag of the drive during the following route through the section profile across bottom strand, return unit and upper run, and reaches its maximum value at the contact with the drive sprocket (Figure 6).

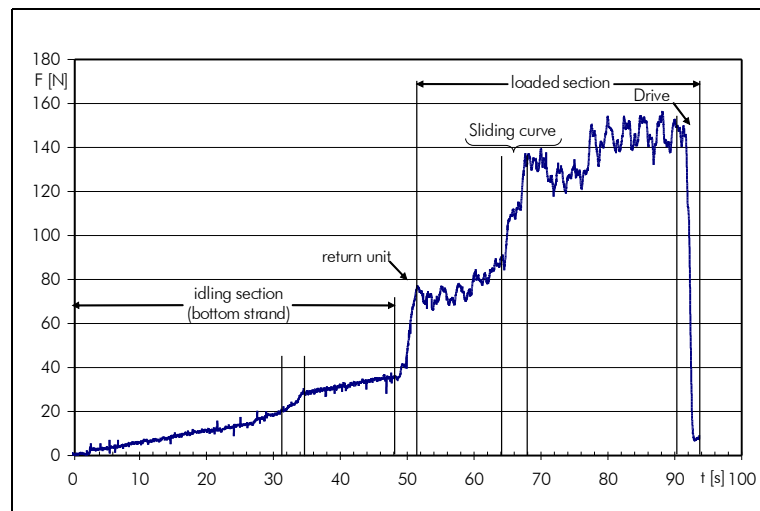


Fig. 6: Chain traction force during a complete circulation

In the diagrammed progression of traction force, explicit segments with diverse increase can be discerned and related to the different track sections. The straight sections cause a linear traction force rising, whereas the sliding curve causes a disproportionate increase. With the approach to the drive, oscillations superimpose the force progression cumulative, which arise because of the polygon effect of the drive sprocket. It follows a presentation of the characteristics of individual section elements as well as the effect of friction co-efficient, speed and traction force.

4.1 Straight sections

The already mentioned linear force rising in straight sections is determined by the specific weight of chain and material being conveyed as well as on the friction co-efficient between chain and slide bar. Crucial for the further course from a considered point, is thereby the increase of the total of transported weight. This is made clear in Figure 7, with the curves of the three leading cases: idling speed, accumulation mode and the transport of the product.

Both, in the idling as well as in the accumulation mode, no cargo will be added, so that the chain traction force is increasing with a small rising, which is determined by the dead weight of the chain. Yet, this rising is not affected by the size of the already existing chain traction force. If one applies weights in constant intervals onto the circulating chain to simulate the transport of cargo, arises the tiered course of the red curve in Figure 7. Would one apply ever smaller weights in shorter distances, a linear course would arise again, but with a higher increase as if without newly added weights.

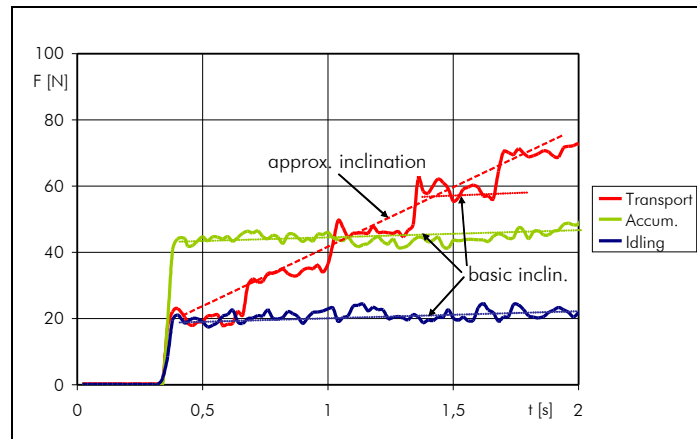


Fig. 7: Traction force progression in straight sections

4.2 Horizontal sliding curve

The course of the tension force in horizontal sliding curves shows an exponential increase. The increase of force is therefore not only dependent from the added weight, but also from the chain tension force at the beginning of the curve. The latter becomes clear, when comparing the curves in idling and accumulation mode in Figure 8.

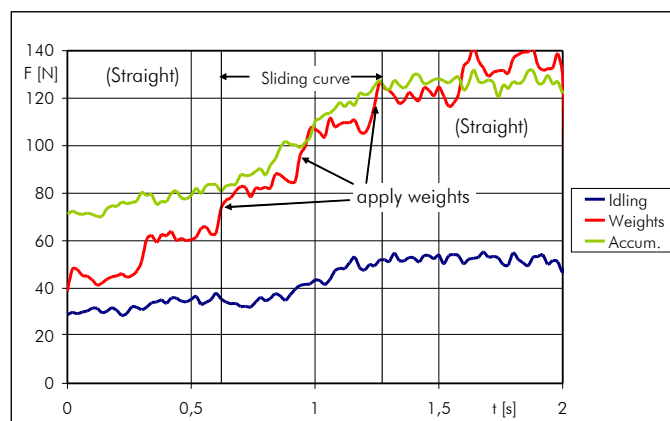


Fig. 8: Tension force progression in horizontal curves

In both cases, no further weight is added after starting the measuring, but the higher starting tension force, due to the accumulation mode, leads to a steep rise of the further force progression as well as to a higher increase of force altogether. While adding weight, jumps can be registered which, averaged, produce a stronger (exponential) increase than with coasting chain.

4.3 Curve Wheels

Curve wheels will be passed through very quickly by the measuring chain link, because of their relatively small radius respectively circumference. Even with lower conveying speed of about 5 m/min, the available period is not enough to add more cargo, so that a simulation of the cargo transport could not be done. Instead, the force progression at multiple starting tension forces was charted, as shown in Figure 9.

In the diagram force peaks at the beginning and end of the curve wheel are apparent – they are an indicator to the multiaxial strain, which is caused through the friction force between pin and lug during the sideways swivelling in and out (cf. chapter Stress Model). After leaving the curve, the chain tension force remains the same, as it would have been in a straight section. The increase of force in curve wheels is also not depending on the initial tension force.

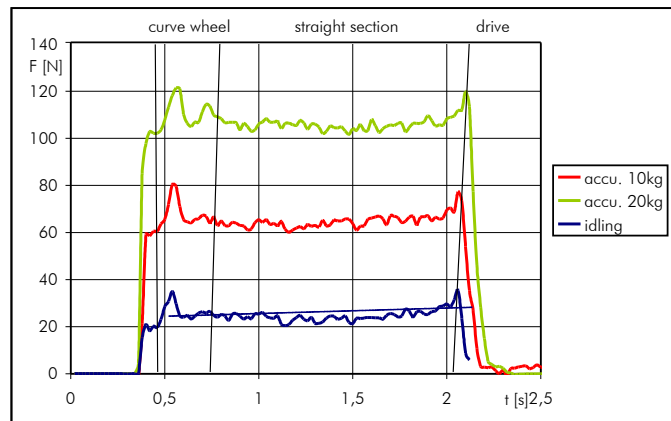


Fig. 9: Tension force progression of curve wheels

4.4 Impact of the conveying speed

In the examined speed range of 5 to 40 m/min, no significant impact of the conveying speed onto the tension force progression could be observed. The friction co-efficient of the examined material matching (Delrin / PE UHMW and Delrin / PVDF) are evidently, in this range of speed, largely constant. The force progressions, acquired with different speeds, are, with otherwise the same conditions, just chronological scaled and could be brought to congruence due to expansion respectively compression.

4.5 Impact of the coefficient of friction

The impact of the coefficient of friction is most obvious in sliding curves, because of the additional occurrence of curve friction. The matchings Delrin-chain contra PE-UHMW as well as PVDF slide rails have been examined, for whom friction co-efficients of 0,26 and 0,15 have been acquired.

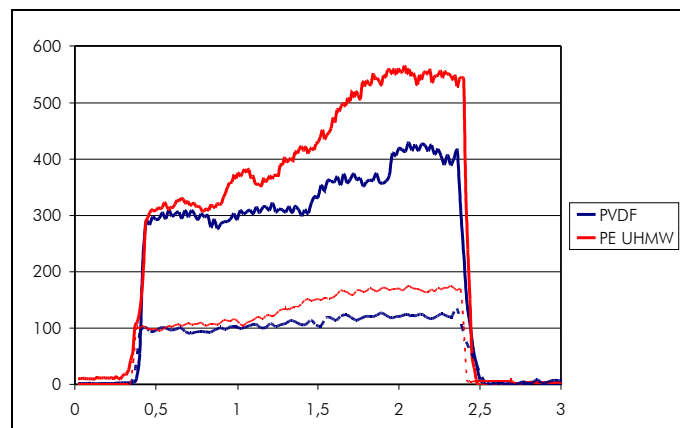


Fig. 10: Impact of the coefficient of friction

The higher coefficient of friction of the PE-slide rails leads, as expected, to a stronger increase of force, which furthermore, is depending in the initial tension force. With the initial tension force of 300 N is the increase of force through the higher coefficient of friction clearly higher as at 100N. This applies only to sliding curves – in straight sections, the increase of force is independent from the initial force. Here, the higher friction co-efficient causes only a bigger linear increase.

5 Calculation of tension forces in sliding curves

The known equation (e.g. [Bosch04]) for straight sections and curve wheels:

$$F_k = F_{k-1} + L \cdot \mu \cdot (q_c + q_p) \quad (1)$$

describes the linear increase of force with sufficient precision. Since the friction forces in sliding curves influence one another through the weight of cargo and chain and the friction in the curve, the exact calculation of the chain tension force has not been possible offhand, so far [Monsberger-79]. Therefore, so-called curve factors K_α are employed (e.g. in [Rexnord00], [FlexLink99] and [Flexon03]), to calculate the increase of force through sliding curves approximately:

$$F_k = [F_{k-1} + L \cdot \mu \cdot (q_c + q_p)] \cdot K_\alpha \quad (2)$$

Frequently, those factors, virtually only valid for a defined friction co-efficient between chain and slide rail, will be indicated flat for all material matchings, so that, depending on the actual friction co-efficient a more or less big error of the tension force is resulting. Furthermore, the impact of the curve radius is ignored, which can cause noteworthy additional tension forces, especially with high specific cargo weights. To overcome these problems, new equations, starting from the balance of forces at a (infinitesimal) piece of chain (Figure 11), have been derived for horizontal and vertical sliding curves.

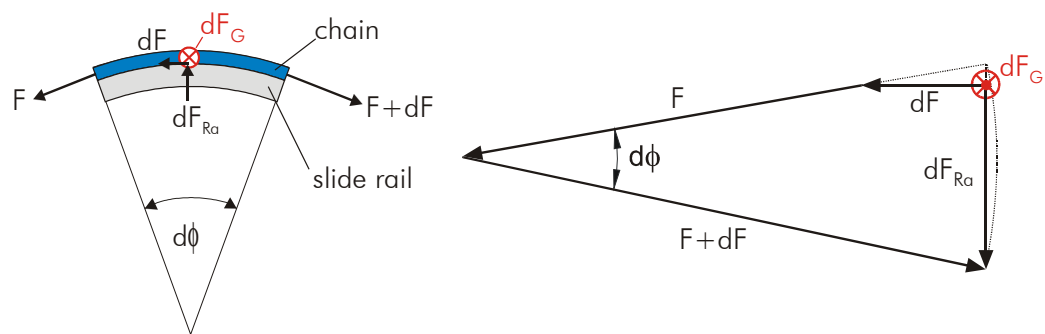


Fig. 11: Forces at the cam segment, force diagram

It follows an outline of the derivation at the example of the horizontal sliding curve. The change of the tension force dF results out of radial force ratio and weight ratio and the friction co-efficient μ :

$$dF = \mu \cdot (dF_{Ra} + dF_G) \quad (3)$$

To evaluate the radial force, the simplifications $\sin d\phi \approx d\phi$ and $dF \cdot d\phi \approx 0$ have been conducted, which are valid for the infinitesimal $d\phi$. The radial force dF_{Ra} is acquired with:

$$dF_{Ra} = F \cdot d\phi \quad (4)$$

The change of the weight-force dF_G results from the arc length and the specific weight-force $q = g \cdot (q_c + q_p)$ of cargo and chain:

$$dF_G = r \cdot q \cdot d\phi \quad (5)$$

After applying (3) and (4) in (5) and rearranging one acquires:

$$\frac{dF}{F + r \cdot q} = \mu \cdot d\phi \quad (6)$$

Equation (6) can be integrated using the following correlation:

$$\int \frac{dx}{x+a} = \ln(x+a) \quad (7)$$

The integration of both sides in equation (6) leads to:

$$\int_{F(\phi_0)}^{F(\phi)} \frac{dF}{F + r \cdot q} = \ln(F + r \cdot q) \Big|_{F(\phi_0)}^{F(\phi)} \quad \text{und} \quad \int \mu d\phi = \mu \cdot \phi \quad (8), (9)$$

After insertion of the limit and exponentiation of both sides to the basis e emerges:

$$\frac{F(\phi)+r \cdot q}{F(\phi_0)+r \cdot q}=e^{\mu \phi} \quad (10)$$

Now the section subscript k is introduced to identify the section limits in the following manner:

$$F(\phi)=F_k \quad \text{und} \quad F(\phi_0)=F_{k-1} \quad (11), (12)$$

and equation (10) is rearranged to get the wanted tension force F_k at the end of the section:

$$F_k=(F_{k-1}+r \cdot q) \cdot e^{\mu \phi}-r \cdot q \quad (13)$$

After reinsertion of $q=g \cdot (q_c+q_p)$ the final form of the new equation is achieved:

$$F_k=\left[F_{k-1}+r \cdot g \cdot (q_c+q_p)\right] \cdot e^{\mu \phi}-r \cdot g \cdot (q_c+q_p) \quad (14)$$

With equation (14) the increase of tension force through horizontal sliding curves can be calculated exactly for any initial power F_{k-1} , friction co-efficient μ and curve radius r . A comparison with measured force progressions produces a good conformity with the calculated force progression according to equation (14), as Figure 12 shows.

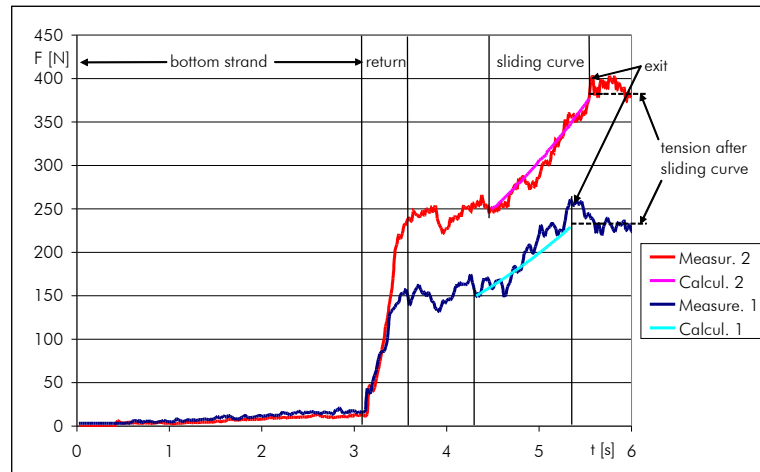


Fig. 12: Comparison measurement / calculation

In a similar way, a new equation has been derived for vertical sliding curves:

$$F_k=\left[\frac{F_{k-1}-r \cdot g \cdot (q_c+q_p) \cdot (\sin \phi_0-\mu \cdot \cos \phi_0)}{e^{\mu \phi_0}}\right] \cdot e^{\mu \phi}-r \cdot g \cdot (q_c+q_p) \cdot (\sin \phi-\mu \cos \phi) \quad (15)$$

A demonstration of the derivation has been excluded to limit the extend of this article. The shown equations are applicable onto further conveyor systems, which are using a loaded chain or different tension element (e.g. modular belt, circular belt, belts, ropes with flat top, or similar), that is in a similar way affected by curve friction. This could also be shown by a comparison congruence with the calculation model for baffle plate conveyors in [Krause99], which relates to the most common case of an arc or a curve, that lies on an arbitrary (spatially) inclined plane.

6 Summary and Outlook

Tension force and strain in side-flexing slide chains are strongly depending on the construction of the conveyor. The most important difference lies between the uniaxial tensile stress in straight sections on the one hand and a complex, multiaxial strain in horizontal curves on the other hand.

New equations have been introduced to allow a more exact calculation of the tension force in sliding curves. The equations can also be applied to similar chains of other conveyor systems. In contrast to the previously used curve factors, the influence of all relevant parameters, such as friction co-efficient, curve radius, and specific weights, can now be taken into account accurately. Measured force progressions in sliding curves could be described appropriately with the new equations.

In a further publication named “Analysis and calculation of durability of 3D plastic slide chains”, effects of different cases of stress onto the durability of slide chains will be described. For that purpose, comparative tests on a dynamic material testing machine as well as on a test conveyor with variable routing will be described. Further on, an approach will be presented, which allows for a calculated estimation of the durability of slide chains. Finally, a computer program will be introduced, in which the advanced computation base and the acquired strength values are integrated.

7 Symbols

Symbol	Unit	Description
F_0	N	Chain tensile force at rear part of a chain link
F_1	N	Chain tensile force at the front of a chain link
F_G	N	Weight of chain and cargo
F_k	N	Chain tension force at the beginning of a section
F_{k-1}	N	Chain tension force at the end of a section
F_{Ra}	N	Radial force
F_{RK}	N	Frictional force in sliding curve
g	m/s ²	Gravitational constant
K_α	-	Curve factor
L	m	Length of the section
q_c	kg/m	Weight per m of the chain
q_p	kg/m	Weight per m of the cargo
r	m	Curve radius
ϕ	-	Angle of Curve
ϕ_0	-	Lead angle at the beginning of a vertical curve
μ	-	Coefficient of sliding friction between chain and slide rail

8 Bibliography

- [Bosch04] Firmenschrift Bosch, VarioFlow Kettenfördersystem, 2004
- [Auerbach06] P. Auerbach, K. Nendel: Investigation and calculation of the durability of side-flexing polymer chains. In: Logistics Journal (2006) ,
- [Monsberger79] Monsberger, Josef: Tragkettenförderer sind vereinfachte Bauformen von Plattenbandförderern. In: Maschinenmarkt 65 (1979) , 1272
- [Rexnord00] Firmenschrift Rexnord, Konstruktionsanleitung Scharnier- und Plattenbandketten, 2000
- [FlexLink99] Firmenschrift FlexLink, Modulares System XT, 1999
- [Flexon03] Firmenschrift Flexon, Produktprogramm Stahl- und Kunststoffketten, 2003
- [Krause99] Krause, F. et.al.: Theoretische und experimentelle Untersuchungen an Stauscheibenförderern (Rohrkettenförderern). In: Schüttgut 2 (1999) , 139-149